Chapter 4
Experimental Methods in Tribology

Nicholas X. Randall

Abstract In order to conduct an accurate tribological investigation of two materials in sliding contact, a dedicated machine or *tribometer* is required which can measure both the friction and wear between the materials. A carefully selected tribometer configuration can be used to simulate all the critical characteristics of a certain specific situation or can be used as a quick way to screen various candidate materials before subjecting them to that situation. This chapter focuses on basic experimental methods as well as the most common test configurations. A good knowledge of tribometers will allow the engineer to choose the most appropriate system to fulfil requirements. Additional knowledge of the environment in which the test should be performed will aid the engineer in simulating true *in-service* conditions which will make the data produced more meaningful. Such conditions (e.g. temperature, humidity, gaseous environment) can then be combined with actual experimental conditions (applied load, sliding speed, contact pressure, etc.) to provide a focused and useful experiment.

1 Fundamentals of Experimental Tribology

Although the fundamentals of tribological testing are beyond the scope of this chapter and more fully covered in other sources [1–3], some basic explanation of the concepts will aid in the understanding of subsequent sections.

Tribology encompasses the study of friction and wear when two materials slide over each other. For two materials in dynamic contact, the coefficient of friction, μ, is defined as the ratio of the tangential force, F_t, and the normal force, F_n, as follows:

N.X. Randall (✉)
CSM Instruments SA, Peseux, Switzerland
e-mail: nra@csm-instruments.com

$$\mu = \frac{F_t}{F_n}$$

The basic laws of friction can be summarized as follows:

1. The tangential force is proportional to the normal load.
2. The tangential force is independent of the apparent area of contact.
3. The tangential force is independent of sliding velocity.

However, it should be noted that such laws are only a guide and have notable exceptions. For example, the first law is well obeyed by most metals and ceramics, but not by polymers which are often in elastic contact and exhibit high viscoelasticity. The third law is applicable once the velocity is high enough to initiate sliding, but the tangential force required to initiate sliding is usually greater than that necessary to maintain sliding. It is therefore common practice to distinguish between the coefficient of static friction, μ_s, and the coefficient of dynamic friction, μ_d. When quoting a friction coefficient value between two materials, one usually refers to the dynamic value.

2   Test Configurations and Equipment

Instrumentation and equipment for tribology testing of materials can be either commercially acquired or built to suit a specific application or a particular in-service condition which is to be simulated. In many cases, a commercially available machine may be adapted relatively easily to various environmental conditions (i.e. liquid sample submersion, heating to body temperature). Some of the most common tribometer test configurations are shown in Fig. 4.1 and have evolved from the need to be able to simulate specific *in-service* conditions which are to be simulated. Tribometers are usually designed for specific wear conditions (e.g. reciprocating sliding) or wear mechanisms (e.g. abrasive wear) and are often ill-suited for experimental conditions which are outside of their intended operating range. Invariably, a tribometer will consist of two or more *wear partners*, where one is usually static and the other(s) is sliding. The applied load between the *static* partner and the *dynamic* partner will usually be applied either by dead weights or by some form of load actuation, and both these systems have advantages and disadvantages. For example, a dead weight system will accurately provide a specific load without any drift or variation, whilst a load actuator can utilize a force-feedback loop which enables a constant load application even when the counterface is rough or has poor flatness. A load actuator is often advantageous when using high speeds and small amplitudes (commonly known as a fretting wear apparatus) as it can better control the load over such short and reversible cycles.
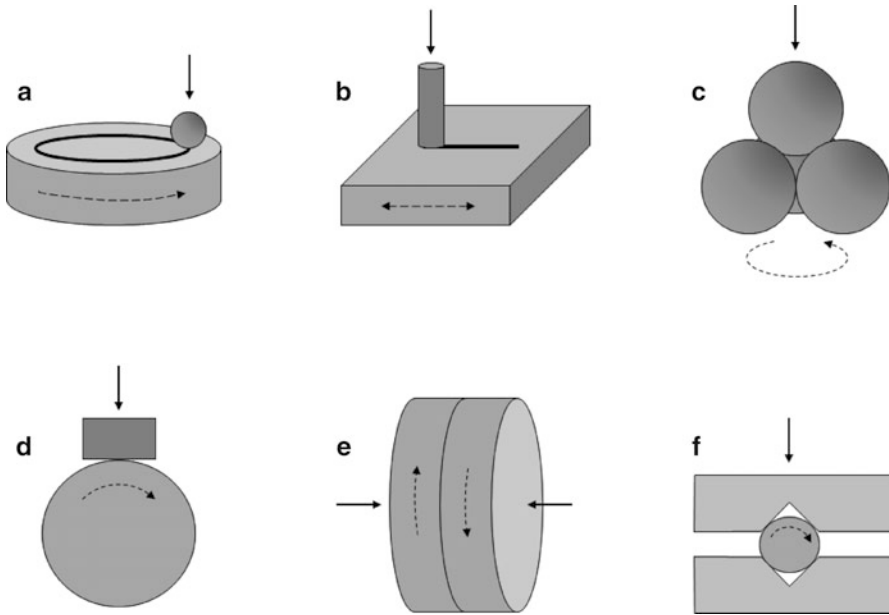
Fig. 4.1 A selection of common tribometer configurations where applied load is denoted by *solid arrows* and motion is denoted by *dotted arrows*; (**a**) ball-on-disk, (**b**) reciprocating pin-on-flat, (**c**) four-ball, (**d**) block-on-wheel, (**e**) flat-on-flat, (**f**) pin and vee-block

2.1 Pin-on-Disk Tribometer

The most commonly used configuration for testing materials is the pin-on-disk method in either rotating or linear-reciprocating modes. The corresponding ASTM standards, G99 [4] and G133 [5], include the measurement of friction coefficient as well as wear rate of the sample and the static partner. The pin-on-disk setup has been used for nearly 50 years for the reproducible measurement of friction and wear [6–12]. The basic principle is shown schematically in Fig. 4.2 and comprises a sample mounted in a chuck which is rotated by a motor. This is the *dynamic partner* of the material pair to be tested. The *static partner* is placed in contact with the sample via an elastic arm, and a dead weight or load cell is used to apply a known load to the contact. A tangential force (sometimes referred to as *friction* force) sensor records the friction between the static and dynamic partners. The static partner can be of any appropriate shape but is usually a flat-ended pin or a ball (the ASTM standards specify a 6 mm diameter ball) depending on the contact configuration desired. The vertically mounted pin has the advantage of a constant contact area throughout the test but has the disadvantage of tending to deviate from perfect alignment to the normal axis under the tangential force produced during the test. The ball has the advantage of a perfectly spherical shape which can be rotated
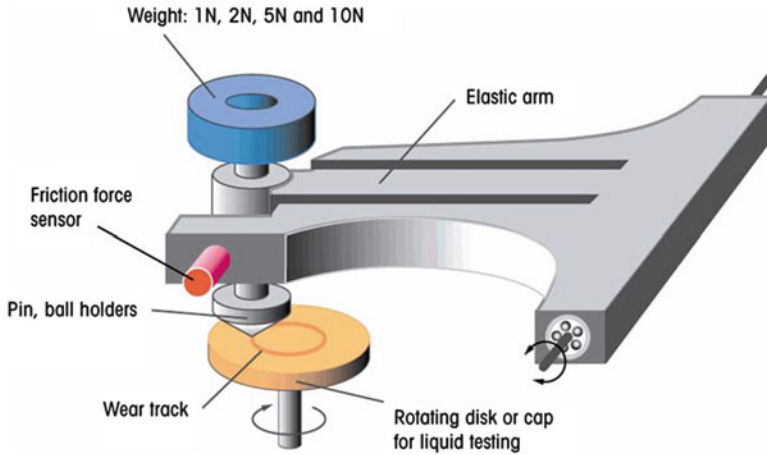
Fig. 4.2 Schematic of the pin-on-disk tribometer

many times so that a fresh area is always used for subsequent tests but has the disadvantage that the contact area will increase as the test progresses.

For some custom applications, both the static and dynamic partners may have specific geometries that simulate a desired condition. For example, when testing prosthetic joint materials, the experimental setup may include a ball (static partner) placed into a conformal cup (dynamic partner) in order to simulate a ball-and-socket configuration.

A typical test might consist of the following steps:

1. Dynamic and static partners mounted and alignment verified.
2. Arm balanced so that dead weight corresponds exactly to desired applied load. Most arms use counterweights to achieve perfect balance.
3. Static partner is brought into contact with sample.
4. Test is commenced and sample begins to rotate at preset speed.
5. Friction signal is recorded as a function of distance, time, or number of laps.

2.1.1   Measurement of Friction Coefficient

An example of a typical friction versus time plot is shown in Fig. 4.3. Most modern instruments will record the raw output of the friction force sensor and will then recalculate the friction coefficient based upon the actual normal load used. Both signals may be recorded. Note in Fig. 4.3 the common *running-in* behaviour as the two surfaces bed into each other, followed by a period of relatively smooth sliding (known as the *steady state*). Such datasets provide two important results:

Steady-state friction coefficient (μ): calculated as the average of the steady-state portion of the trace
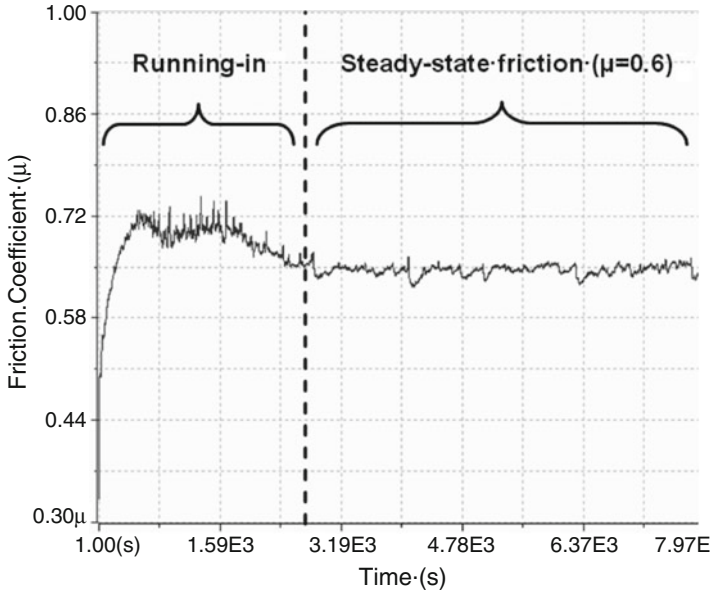
Fig. 4.3 Example of a friction coefficient versus time plot for a steel-on-steel contact

Static friction coefficient: calculated as the maximum value of friction reached during the initial running-in period

It should be noted that the friction coefficient is not a material property but a measured parameter which is highly dependent on the environmental conditions. For example, the coefficient of friction measured during a dry winter day (15 % RH) may be very different to that measured on the same material pair during a humid summer day (85 % RH). For this reason, it is very important to record the exact environmental conditions (temperature and humidity) during which the test was performed.

The duration of the tribology test will depend on whether the user only wants to measure a value of friction coefficient (in which case the test duration will be only up until steady-state conditions are reached) or whether the evolution of wear is of interest. In the latter case, the test duration may be for extended time periods, typically from several hours to several days, depending on the severity of the test conditions. In some cases, the test may be continued until one or both of the material pair are completely destroyed, such a condition being characterized by a very high friction value or even seizure of the contact. The time from test initiation to catastrophic failure may give an idea of the lifetime of the tested material pair and may be used to screen new materials using conditions which accelerate breakdown of the contact.
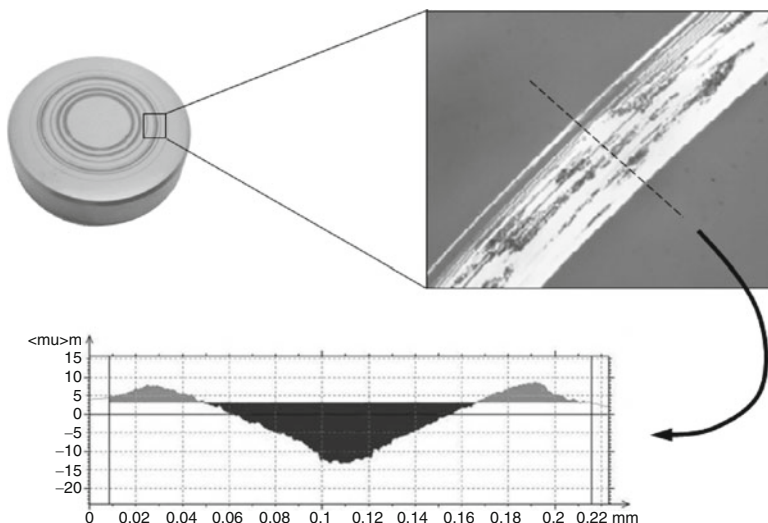
Fig. 4.4 Typical wear track section measured using a stylus profilometer

2.1.2 Measurement of Wear Rate

If sufficient material is removed during the test which is measurable, then the wear rates of both the dynamic and static partners can be calculated. The simplest method is to weigh both partners before and after the test and thus calculate the mass of material removed. However, if the material lost is so small as to be immeasurable using conventional techniques (e.g. high-resolution mass balance), then the amount of material lost must be directly calculated. In the case of the dynamic partner (usually a flat disk), it is relatively easy to measure a profile across the wear track using a profilometer (either stylus or optical), from which the area of the wear track section can be calculated. The volume of material lost is then calculated by multiplying the area by the circumference of the wear track. Figure 4.4 shows a typical example of such a measurement, and it should be noted that at least three profiles are usually measured per wear track and an average value used to calculate volume.

Some tribometer software packages automatically convert the worn track section (μm^2) into a volume loss (μm^3) and a wear rate (in $mm^3 N^{-1} m^{-1}$).

The wear rate of the static partner is calculated in the same way but depending on the actual geometry. For a ball, the worn cap diameter can be measured using a calibrated microscope as shown in Fig. 4.5. The height, h, of the worn cap is given by

$$h = R - \sqrt{R^2 - \frac{d^2}{4}}$$

where R is the radius of the ball and d is the diameter of the worn cap.

Fig. 4.5 Worn cap diameter as viewed in a scanning electron microscope (SEM)
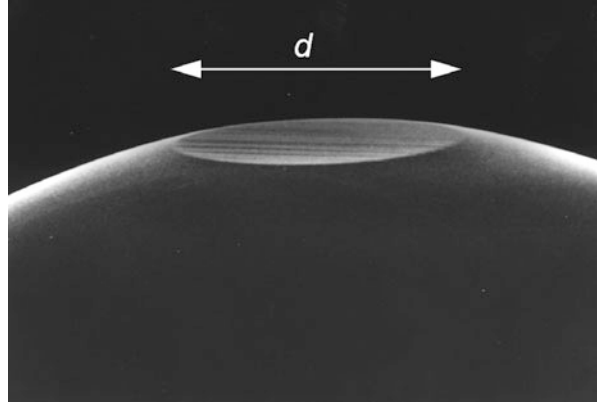
The volume, V, of the worn cap is then

$$V = \frac{1}{3}\pi h^2 (3R - h)$$

And the wear rate of the static partner is thus

$$WearRate_{StaticPartner} = \frac{V}{L.F_n}$$

where L is the distance travelled during the test and F_n the applied normal load.

When measuring the tribological properties of thin films and coatings, the minimum measurable mass loss is approximately 3 mg, if measured by conventional techniques such as a high-precision mass balance. For most engineering situations where coatings are employed, the actual mass loss may be significantly less than this threshold value. The data in Fig. 4.6 shows mass loss as a function of coating thickness for a range of common coatings where any mass loss below 3 mg must be calculated by the aforementioned indirect methods.

If investigating the evolution of friction and wear over the lifetime of the material pair, it may be interesting to pause the test at various intervals and look at the wear track through a microscope, as shown in Fig. 4.7. Such online analysis permits changes in wear mode to be detected, e.g. transition from abrasive to adhesive wear, and can help in understanding variations in the friction coefficient over the lifetime of the contact.

A summary of a complete dataset is shown in Fig. 4.8 for a ball-on-disk experiment performed in dry conditions. The friction signal has steadily increased over the lifetime of the contact as the debris produced from adhesive wear has created a third-body transfer film which has then, in turn, caused increased wear of both partners. The wear rates of the sample (disk) and the static partner (ball) have been calculated after having entered the worn track section and the worn cap
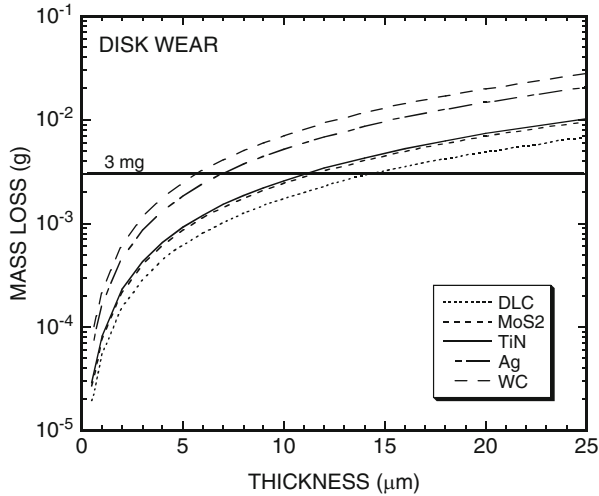
Fig. 4.6 Mass loss versus thickness for a range of coating materials
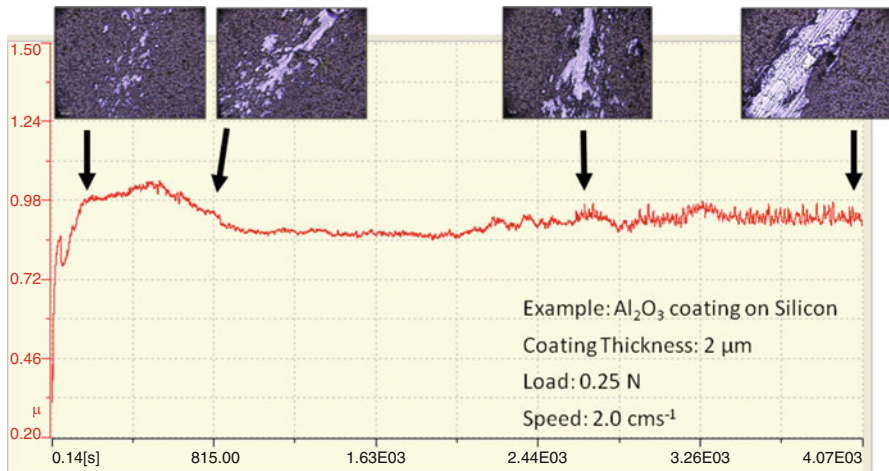

Fig. 4.7 Evolution of wear for an alumina coating in contact with a 100Cr6 steel ball

diameter, respectively. In addition, the maximum stress at the contact has also been calculated and displayed. In many applications, it may be necessary to use a suitable size ball which gives the approximate stress which the components may see in service. This is another advantage of using the ball-on-disk configuration instead of the pin-on-disk where it is much harder to fabricate suitable pins.
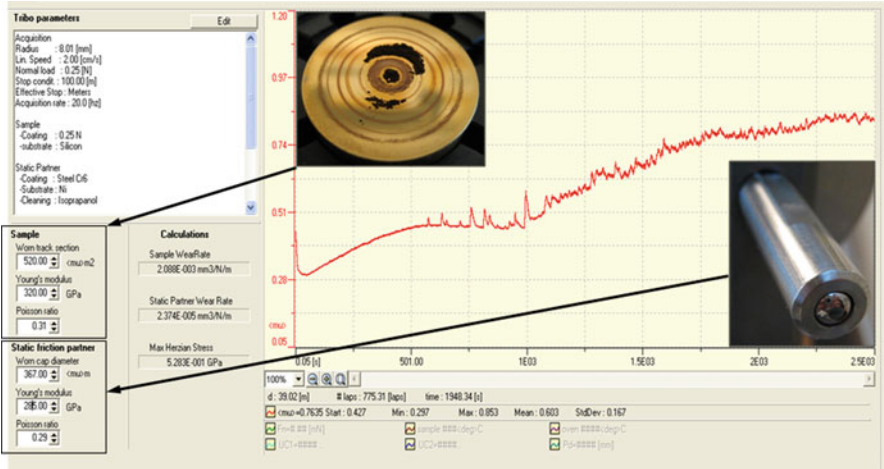
Fig. 4.8 Typical ball-on-disk results window from a commercial tribometer with (*inset*) images of wear debris produced on the disk and the ball

2.1.3 Tribocorrosion

The term "tribocorrosion" is defined as a material degradation process which is due to the combined effect of corrosion and wear, and it is common to describe the combined process as *corrosion-accelerated wear* or *wear-accelerated corrosion,* depending on how one views the process [13].

Whilst tribocorrosion phenomena may affect many materials, they are most critical for metals, especially the normally corrosion-resistant so-called passive metals. The vast majority of corrosion-resistant metals and alloys used in engineering (stainless steels, titanium, aluminium, etc.) fall into this category. These metals are thermodynamically unstable in the presence of oxygen or water, and they derive their corrosion resistance from the presence at the surface of a thin oxide film, called the *passive film*, which acts as a protective barrier between the metal and its environment [15]. Passive films are usually just a few atomic layers thick. Nevertheless, they can provide excellent corrosion protection because if damaged accidentally they spontaneously self-heal by metal oxidation. However, when a metal surface is subjected to severe rubbing or to a stream of impacting particles, the passive film damage becomes continuous and extensive. The self-healing process may no longer be effective and in addition it requires a high rate of metal oxidation. In other words, the underlying metal will strongly corrode before the protective passive film is reformed, if at all. In such a case, the total material loss due to tribocorrosion will be much higher than the sum of wear and corrosion one would measure in experiments with the same metal where only wear or only corrosion takes place. The example illustrates the fact that the rate of tribocorrosion is not simply the addition of the rate of wear and the rate of corrosion, but it is strongly
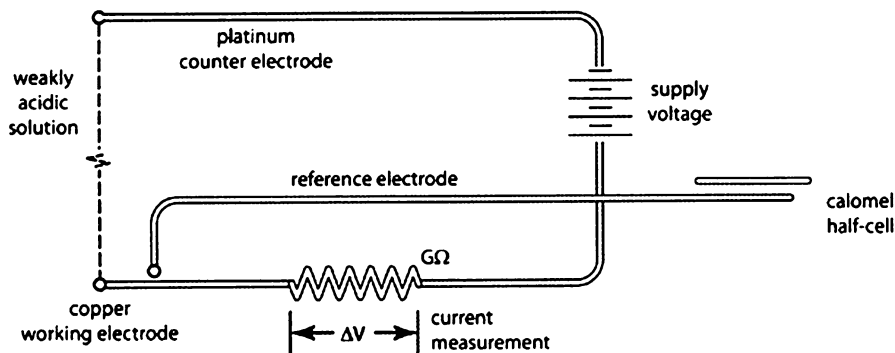
Fig. 4.9 Circuit diagram for a simple tribocorrosion setup

affected by synergistic and antagonistic effects between mechanical and chemical mechanisms. To study such effects in the laboratory, one most often uses mechanical wear testing rigs which are equipped with an electrochemical cell [16]. This permits one to control independently the mechanical and chemical parameters. For example, by imposing a given potential to the rubbing metal, one can simulate the oxidation potential of the environment, and in addition, under certain conditions, the current flow is a measure of the instantaneous corrosion rate. For a deeper understanding, tribocorrosion experiments are often supplemented by detailed microscopic and analytical studies of the contacting surfaces.

In the field of bioengineering, the term "biotribocorrosion" is often used to describe tribological systems exposed to biological environments and has been studied for artificial joint prostheses where an understanding of material degradation processes is key to achieving longer service life for such devices [14].

A practical tribocorrosion setup is shown as a circuit diagram in Fig. 4.9 and includes the following components:

- Sample (disk): this can be the working electrode, or a separate electrode can be placed in the liquid bath.
- Static partner (ball): typically of ceramic (Al_2O_3 or Si_3N_4) in order to be unreactive in a corrosive electrochemical environment.
- Ag/AgCl reference electrode.
- Pt counter electrode (provides stable potential and is corrosion resistant).
- Electrolyte solution (NaCl or body-mimicking fluid).
- Heating coil and thermostat if a stable temperature is required (e.g. body temperature).

Such a setup allows the user to perform wear tests in corrosive environments under well-defined electrochemical conditions and at controlled temperature. The following modes of operation can be used:

Open Circuit Potential (OCP): The free potential is monitored throughout the wear test and indicates changes occurring, e.g. corrosion/passivation of a metal or deterioration of a surface coating characterized by a decrease in the measured OCP.
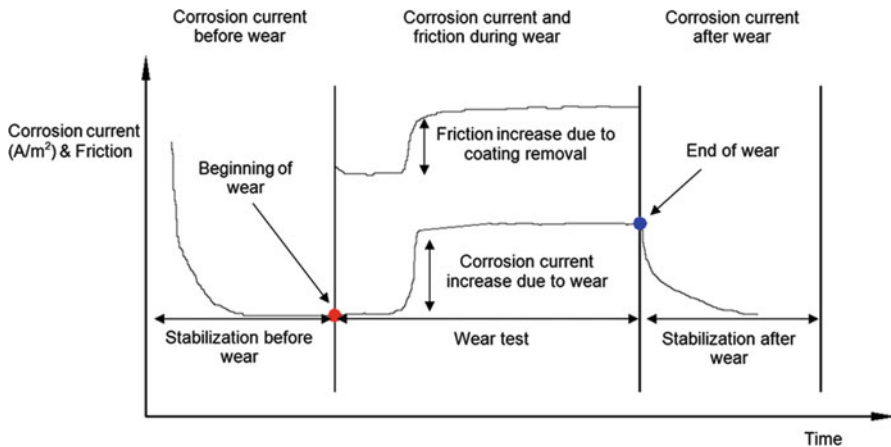
Fig. 4.10 Example of a fixed potential test where the corrosion current is monitored throughout the wear process

Fixed Potential: Also known as potentiostatic wear mode, this involves monitoring the evolution of the corrosion current at different phases in the test whilst maintaining a fixed potential which is chosen to accelerate the corrosion process. An example is shown in Fig. 4.10. This allows investigation of the wear-enhanced corrosion (increased corrosion as a direct result of rubbing) and the repassivation kinetics of the surface. An anodic potential is chosen to accelerate corrosion, whereas a cathodic potential is chosen to protect the surface and therefore isolate only mechanical wear at the interface.

Potential Scan: Also known as potentiodynamic wear mode, this allows the friction coefficient to be monitored as a function of the applied potential.

The synergy between corrosion and wear can be evaluated over wide ranges of both electrochemical and mechanical conditions [17–19]. Experimental setups will depend on the complexity of the system which is to be modelled and the aggressiveness of the electrolyte used [20–22]. An example of a tribocorrosion tribometer is shown in Fig. 4.11.

2.1.4 Electrical Contact Resistance (ECR)

In certain tribological situations, it may be of interest to monitor changes in electrical contact resistance (ECR) over the duration of a friction test. Changes in ECR can be used to detect the onset of failure in thin biomaterials which have been coated onto a conducting substrate (e.g. polymer coatings on heart valves, drug-eluting coatings, and pacemaker device packaging).

A typical ECR experimental arrangement is shown in Fig. 4.12 which enables an open circuit to be created between the static partner and the coated disk, with the coating acting as an insulating electrical barrier. As the static partner wears through

Fig. 4.11 Schematic of a commercial pin-on-disk tribometer modified for tribocorrosion testing with liquid cell and contacts for electrodes
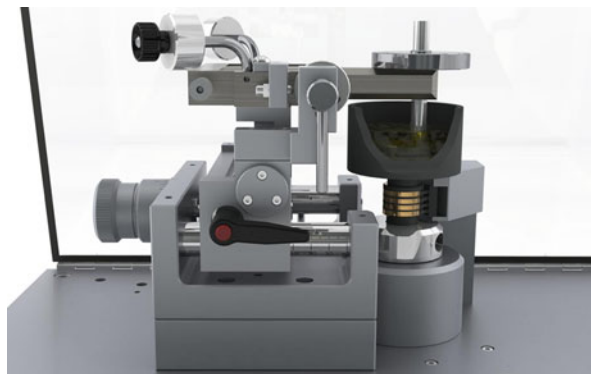
Fig. 4.12 Pin-on-disk tribometer setup for ECR measurement showing the ball holder which is electrically isolated from the system
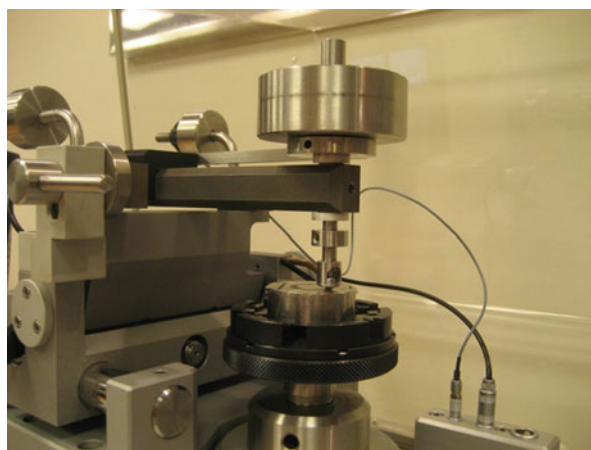

the coating, changes in the measured resistance can be recorded simultaneously with the friction signal.

In some cases, a measured change in the ECR signal may correspond to a change in the tribological mode, for example, when a transfer film is built up from particles of the static partner mixing sufficiently with material from the insulating coating to cause current to pass. An example of a typical ECR test is shown in Fig. 4.13 for a polypropylene coating deposited on a polished steel substrate. Note that in this example the measured drop in contact resistance does not correspond to a marked transition in the friction signal.

2.1.5 Linear-Reciprocating Motion

In some cases, the friction/wear condition which is to be simulated may not correspond to a rotating pin-on-disk configuration and may be closer to a linear-reciprocating motion. Examples of the latter might be the deployment of a stent into
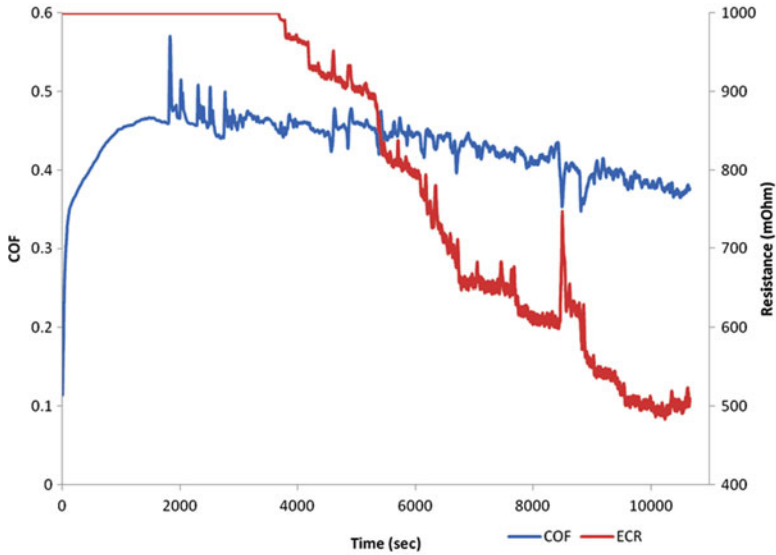
Fig. 4.13 Coefficient of friction (COF) and electrical contact resistance (ECR) plotted as a function of time for a 100Cr6 steel ball in contact with a polypropylene coating

Fig. 4.14 Experimental configuration for linear-reciprocating motion
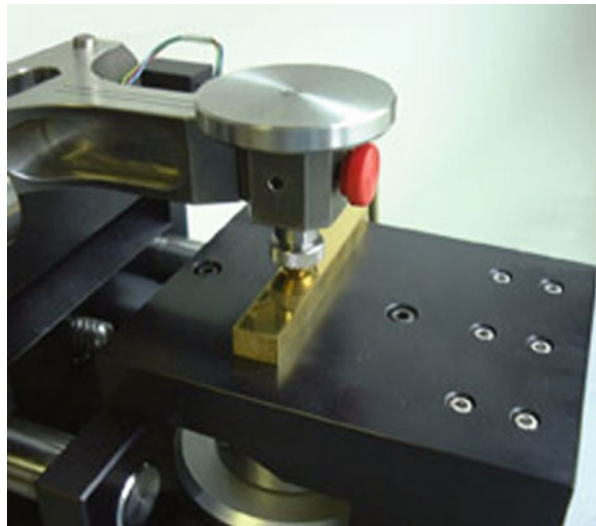
an artery, a contact lens moving over the cornea, or the movement of a catheter. The basic pin-on-disk setup remains the same but the dynamic partner is reciprocated rather than rotated, as shown in Fig. 4.14.

The amplitude of the linear stroke (or stroke length) can usually be varied as well as the frequency of reciprocation in order to simulate in-service conditions in a
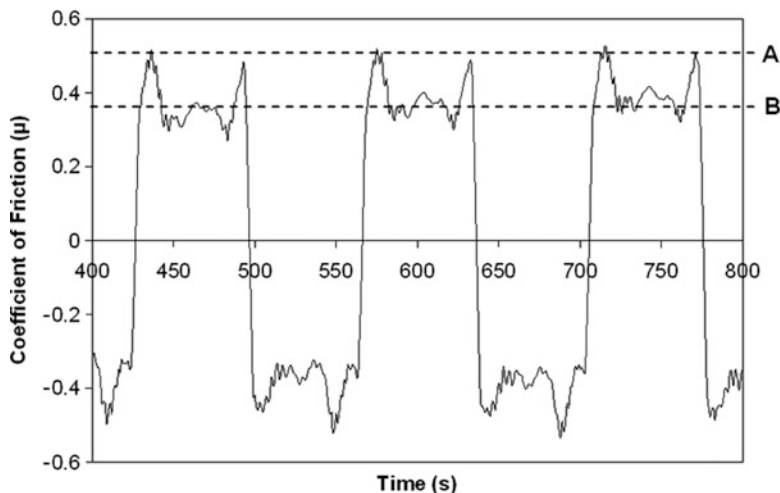
Fig. 4.15 Typical friction coefficient trace for a steel-on-steel contact showing the coefficient of static friction (**a**) and the coefficient of dynamic friction (**b**) measured from each cycle

controlled manner. Another main difference with a rotating test is that the linear reciprocation means that the tangential force can be measured in both directions and the speed is not constant: the movement accelerates from a standstill on every cycle. This means that the modes of wear may be quite different between a reciprocating test (where the wear debris may be pushed back into the contact zone) and a rotating test (where the sliding direction is always the same and debris tends to be pushed outside of the contact).

Because of the continuous acceleration/deceleration during linear reciprocating, it is possible to extract both the coefficient of static friction and the coefficient of dynamic friction from each cycle and in both directions, as shown in Fig. 4.15.

Modern software packages allow the measured values to be averaged as shown in Fig. 4.16. The user can select a specific point on each successive cycle in one direction (1st way extraction) and the opposite direction (2nd way extraction) and then can calculate an average of the 2 values (2-way extraction). This is a fast way to analyse friction and wear effects at different points in a reciprocating cycle. For example, the friction coefficient at maximum linear speed (in the middle of the cycle) could be compared to the friction coefficient during initial acceleration.

2.1.6   Heated Liquid Testing

Tribological testing in the laboratory allows many complex variables to be investigated individually and in combination with each other. A typical experimental arrangement for evaluating a biomaterial pair in a controlled physiological
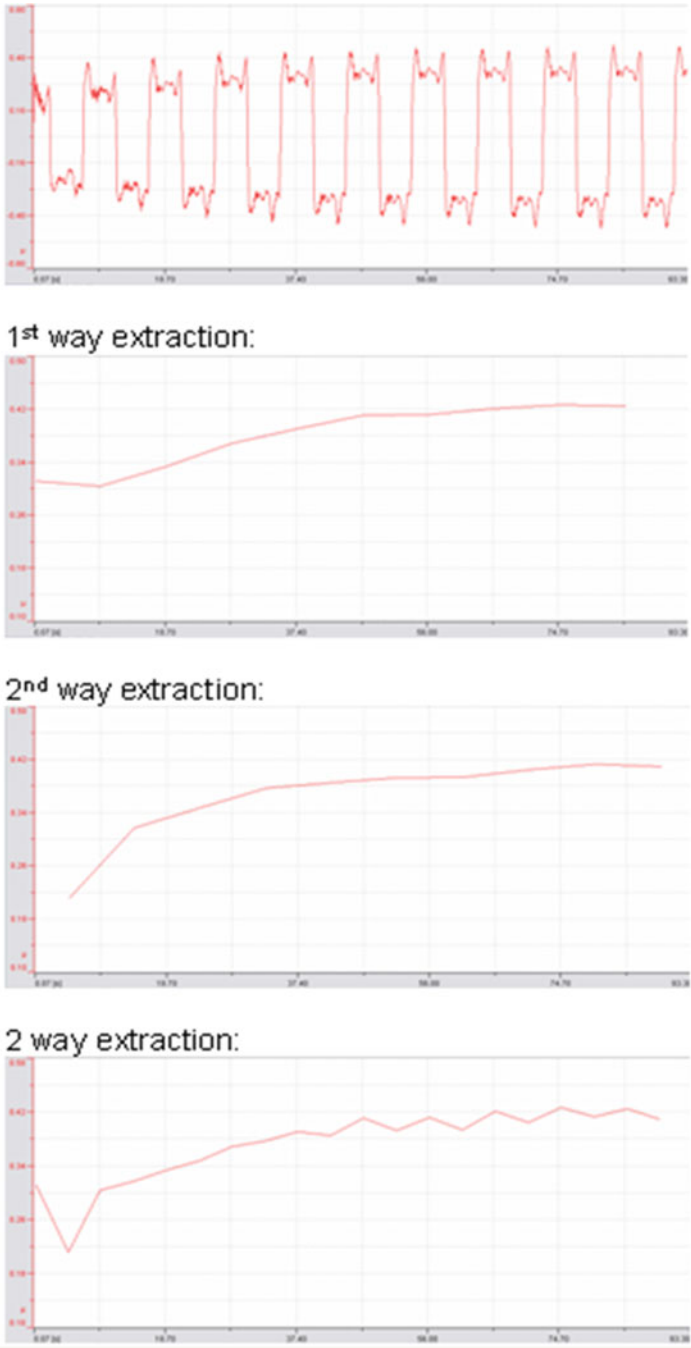
Fig. 4.16 Analysis of a linear-reciprocating dataset (*top*) consists of extracting the same point on each successive cycle in one direction (1st way extraction) and the opposite direction (2nd way extraction) and then averaging the 2 values (2-way extraction)

Fig. 4.17 Experimental
arrangement for pin-on-disk
testing of a biomaterial pair
in simulated physiological
saline solution. Tribological
pair is submerged in a liquid
cup whose contents are
maintained at 37 °C by a
heating coil

environment is shown in Fig. 4.17, where the static and dynamic partner materials
are submerged in a cup containing the body-mimicking fluid (BMF) of choice and
whose liquid temperature is maintained at a constant 37 °C by a submerged heating
coil. This arrangement allows standardized testing to ASTM F-732 [23] with either
rotating or angular reciprocating motion.

A common example of this test configuration is the investigation of fatigue wear
of ultra-high-molecular-weight polyethylene (UHMWPE) for hip implants, where
the UHMWPE ball reciprocates against a flat metallic CoCr counterface. The
counterface is usually in the form of a disk which must be held down by a retaining
ring as shown schematically in Fig. 4.18. This reciprocating tribological test is very
relevant to orthopaedic implants as most bearing surfaces have a reciprocating
motion as opposed to a unidirectional motion. One important consideration is that
the polymeric ball must be presoaked in the BMF to minimize fluid sorption during
the wear test: without presoaking, UHMWPE materials can show a net increase in
weight or volume during the initial wear intervals due to fluid sorption.

2.2   Four-Ball Wear Tester

The four-ball test configuration was originally designed to investigate the antiwear
properties of a lubricant under boundary lubrication (metal-to-metal contact). The
specific configuration ensures that the *extreme pressure* (EP) properties of the
lubricant can be measured under high Hertzian contact and the results can help to
determine the load-bearing properties of the lubricant at high applied pressures. The
test configuration is shown in Fig. 4.19 where three steel balls (of half-inch
diameter) are clamped together to form a cradle upon which a fourth ball rotates

Fig. 4.18 Schematic of the liquid cup used in the arrangement shown in Fig. 4.16, where the flat counterface (disk) must be retained by a sample holder (retaining ring)

Screws

Sample holder

Sample

Lubricant container
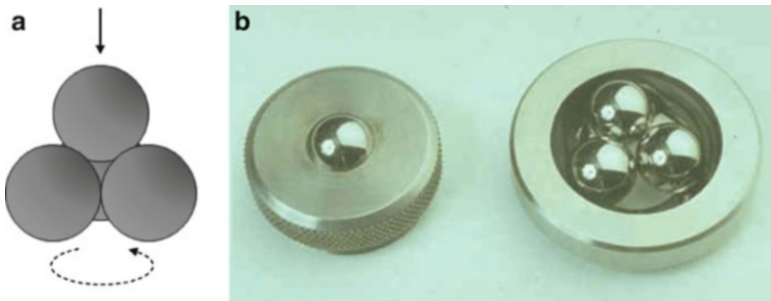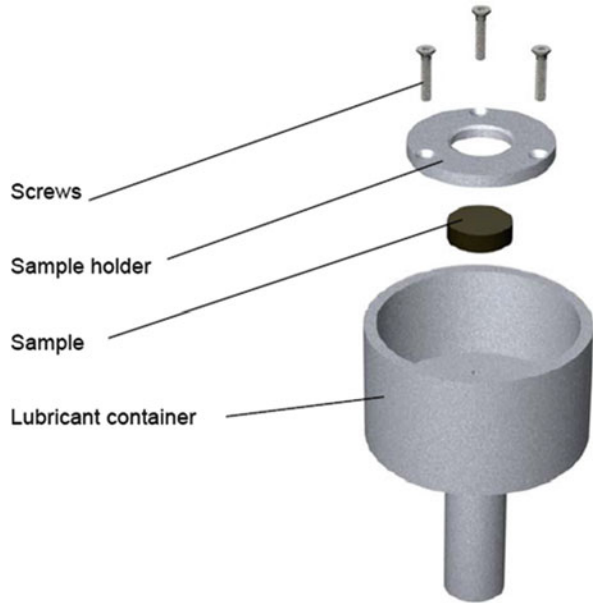
Fig. 4.19 The four-ball test configuration shown schematically (**a**) and the actual test pieces used (**b**)

on a vertical axis. The four balls are immersed in the oil sample at a specified speed, temperature, and load. At the end of a specified test time, the average diameter of the wear scars on the three lower balls is measured, an example of which is shown in Fig. 4.20. During the test, the load is increased every 10 min up to the point where the frictional trace indicates incipient seizure. The coefficient of friction may be measured at the end of each 10 min interval, provided the instrument has the necessary force sensors (see ASTM D5183 test method, [27]). The test is generally terminated at the load at which the rotating ball "welds" to the three stationary balls causing seizure.

Fig. 4.20 Typical example
of a wear scar and the
diameter measurement used
in the wear rate calculation
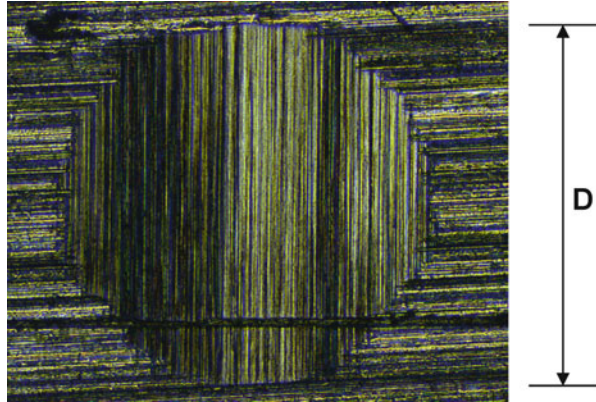
The three most common parameters measured with the four-ball configuration
are as follows:

1. Load-Wear Index (LWI): simple ratio which quantifies the degree of wear
   protection at each test load (often plotted as a function of applied load)
2. Last Non-Seizure Load (LNSL): provides an indication of the point of transition
   from elastohydrodynamic to boundary lubrication and metal-to-metal contact
3. Weld Point (WP): point at which seizure occurs

The most common standards used with the four-ball test configuration are
ASTM D4172 [28] and ASTM D2266 [29].

2.3 Block-on-Ring Tester

The block-on-ring test is commonly used to determine the resistance of materials to
sliding wear by ranking the particular material pair according to its wear
characteristics under various conditions. One important attribute of this test is
that it is very flexible as any material can be tested, as long as it can be fabricated
into blocks or rings with relative ease. The test can be run either dry or with various
lubricants, liquids, or gaseous atmospheres to simulate in-service conditions with
the greatest accuracy.

The actual configuration is shown in Fig. 4.21 and the dimensions of the
test pieces (both block and ring) will depend on the specific standard test
procedure used.

Various machines are commercially available for this test, although they may
differ slightly in lever arm ratio, load range, speed control (variable or fixed), speed
range, and method of measuring friction (if any). In addition to measurement of the
ranking resistance of materials to sliding wear, the block-on-ring method is also
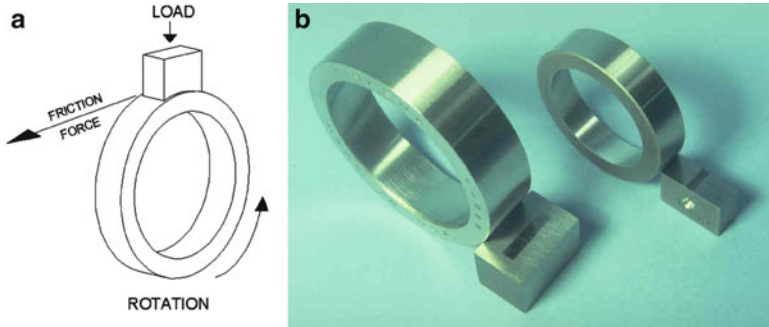commonly used for measuring wear properties and extreme pressure properties of

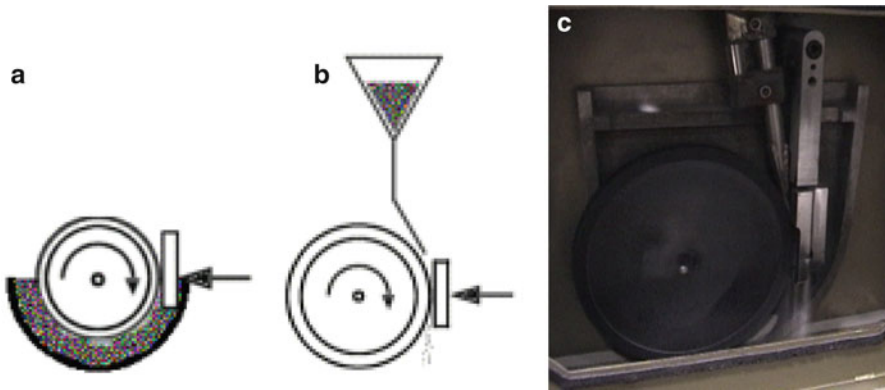**Fig. 4.21** The block-on-ring test configuration shown schematically (**a**) and the actual test pieces used (**b**)

Fig. 4.22 The dry sand abrader test configuration shown schematically (**a**), (**b**), and actual test in progress (**c**)

lubricants and greases. The configuration can also be varied to provide different contact geometries between the test pieces, typically line, area, and point contacts. For a point contact, a ball-on-ring configuration is used.

2.4 Dry Sand Abrader

The dry sand abrader is used to test the abrasive resistance of solid materials to abrasive dry sand compositions. Materials such as metals, minerals, polymers, composites, ceramics, abrasives, and thick coatings can be tested with this instrument. The test is performed by loading a rectangular test sample against a rotating rubber wheel and depositing sand of controlled grit size, composition, and flow rate between them.

Typical test system setups are shown in Fig. 4.22, and the abrasive can be either static (as shown in (a)) or dynamically fed to the interface at a fixed flow rate. In the
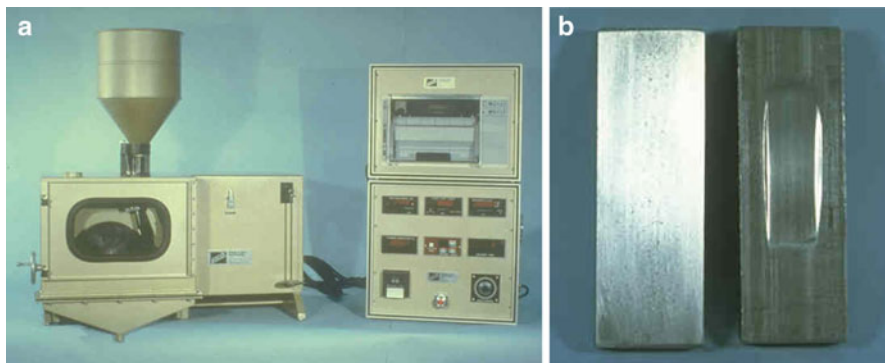
Fig. 4.23 Commercially available dry sand abrader (**a**) together with some typical steel test specimens before and after testing (**b**)

more common ASTM G65 method [30], the wheel, comprised of synthetic rubber of 60 Shore A hardness, is rotated in the direction of the flow of sand. The mass of the test sample is recorded before and after conducting a test, and the difference between the two values is the resultant mass loss due to dry sand abrasion. To develop a comparison table for ranking different materials with respect to each other, it is necessary to convert this mass loss to volume loss to account for the differences in material densities.

The test load and sand composition can be varied. The test parameters can be configured to perform tests as per ASTM G65 specifications. The test simulates what is commonly referred to as Low Stress Abrasion or Scratching Abrasion, both being characterized by the lack of any fracturing of the abrading material. This means that the abrasive sane particles retain their shape and size throughout the test procedure. This is in contrast to High Stress Abrasion or Grinding Abrasion where the sand particles are actually fractured into smaller pieces. Such newly created particles are very sharp and angular and will produce a very different wear mechanism due to the high degree of stress applied.

A typical commercial system for running such tests is shown in Fig. 4.23 as well as some typical test specimens. Weight loss is usually quoted in grams for such sample sizes. This test is an invaluable tool in the ranking of materials and prediction of component wear lifetime.

2.5 Ball Crater Abrader

The ball crater abrader (also commonly referred to as Calotest or Calowear Tester) provides a fast and simple method for measuring the wear coefficient of both bulk and coated materials. The basic principle is shown in Fig. 4.24a where a rotating
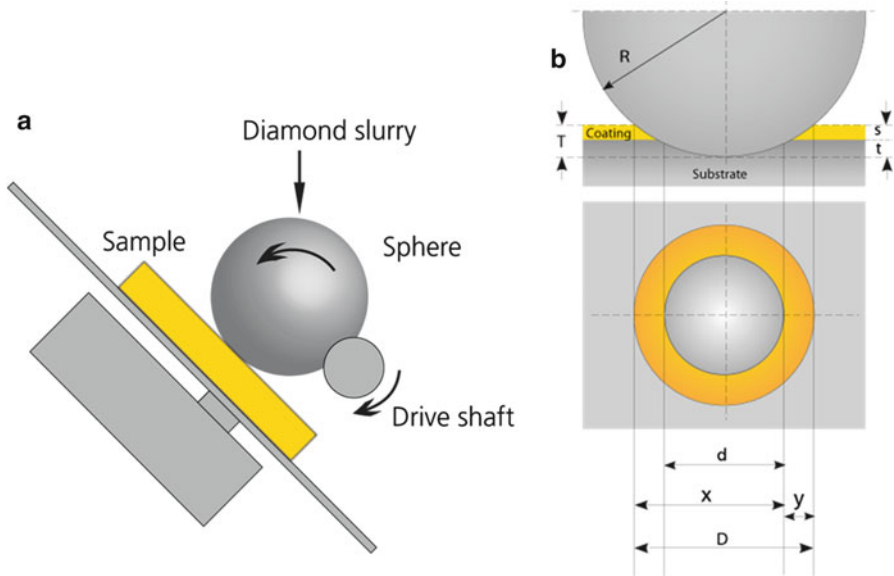
Fig. 4.24 Basic principle of the ball crater abrader (**a**) and summary of calculation parameters when abrading through a coating into the substrate (**b**)

sphere of known diameter is rotated on the sample surface with a preselected load. An abrasive slurry is applied to the contact causing a spherical depression to be produced in the sample. This depression, or ball crater, is also often referred to as a "calotte" and is subsequently viewed under an optical microscope in order to measure its diameter [31]. If the sample is coated, then it is possible to measure the thickness of the coating, s, using the parameters shown in Fig. 4.24b and the following equation:

$$S = \frac{1}{2}\left(\sqrt{4R^2 - d^2} - \sqrt{4R^2 - D^2}\right)$$

In addition, the ball crater technique can be used to calculate the abrasive wear coefficients of either a bulk material or a coating and substrate independently. This approach [32, 33] starts with a simple model for abrasive wear based on the Archard equation [34] which assumes independent wear coefficients for the coating and substrate. Taking into account the experimental geometry, the wear volumes are expressed assuming that the calotte diameter is much smaller than the ball diameter, leading to the following equation for the wear coefficient, K, of a bulk material:

$$K = \frac{\pi b^4}{32LF_N d}$$

where F_N is the normal force on the sample, b is the diameter of the wear crater, L is the sliding distance, and d is the diameter of the ball.

For coated materials, we consider the combined wear of a coating and substrate, each with an independent wear coefficient. Following the methodology of Rutherford and Hutchings [33], the following equation is used to derive the wear coefficients of the coating, K_c, and of the substrate, K_s:

$$\frac{LF_N}{b^4} = \left(\frac{K_S - K_C}{K_S K_C}\right)\left(\frac{\pi h}{4b^2} - \frac{\pi dh^2}{2b^4}\right) + \left(\frac{1}{K_S}\right)\left(\frac{\pi}{32d}\right)$$

Thus, a plot of $Y = \frac{L \cdot F_N}{b^4}$ versus $X = \frac{\pi \cdot h}{4b^2} - \frac{\pi \cdot d \cdot h^2}{2b^4}$ should be linear.
So we can consider this equation as a linear function: $Y = A \cdot X + B$
where

$$A = \frac{K_S - K_C}{K_S \cdot K_C}$$

and

$$B = \frac{1}{K_S} \cdot \frac{\pi}{32d}$$

Experimentally, several values are plotted and then fitted with a straight line which yields A and B, as shown in Fig. 4.25.

The wear coefficients are then calculated using the intercept (B) and the slope (A) as follows:

$$K_S = \frac{1}{B} \cdot \frac{\pi}{32d}$$

$$K_C = \frac{K_S}{A \cdot K_S + 1} = \frac{\frac{1}{B} \cdot \frac{\pi}{32d}}{A \cdot \left(\frac{1}{B} \cdot \frac{\pi}{32d}\right) + 1}$$

Some examples of ball craters on coated materials are shown in Fig. 4.26. In principal, the technique can be used to measure the wear coefficients of each independent coating, even in a complicated multilayer such as in Fig. 4.26b. It should be noted that the minimum coating thickness that can be measured in this manner is approximately 200–500 nm, depending on the quality of the interface and the optics used to measure the dimensions.

Commercially available equipment for measuring ball crater abrasion is shown in Fig. 4.27, in this case the Calowear Tester from CSM Instruments. The experimental arrangement is clearly shown in Fig. 4.27b and the load cell provides a direct acquisition of the normal load applied by the ball on the sample. In practice, this load can be varied by changing the lateral position of the motor drive shaft. The abrasive slurry is automatically fed to the ball/sample interface by a feed pump and flexible tubing. The resultant calottes are viewed through an integrated optical microscope which provides direct measurement of the ball crater dimensions.
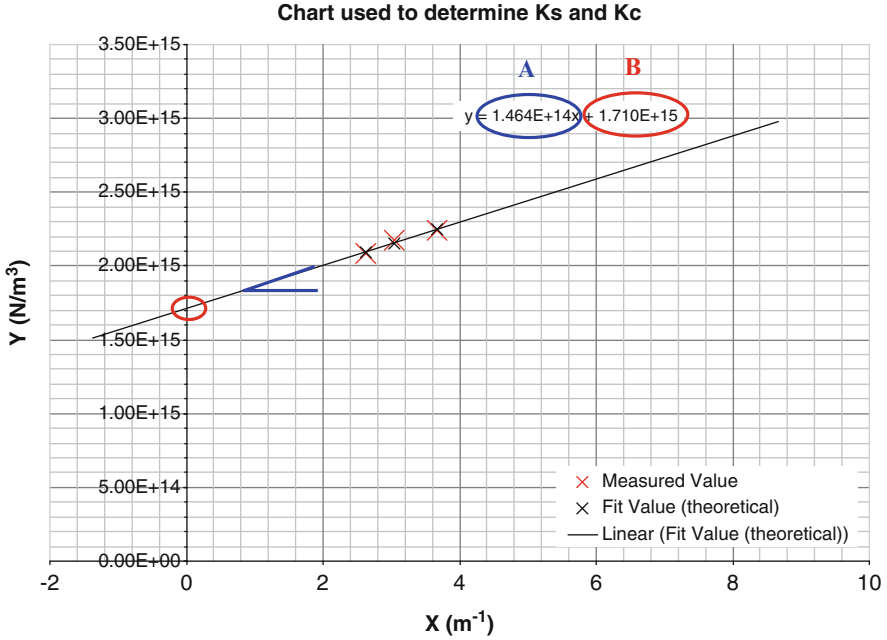
Fig. 4.25 Typical example of a plot from which the coating and substrate wear coefficients are derived for a TiN coating on a 440C steel substrate. The *crosses* show the actual experimental points made with a CSM Instruments Calowear Tester, to which the straight line has been fitted
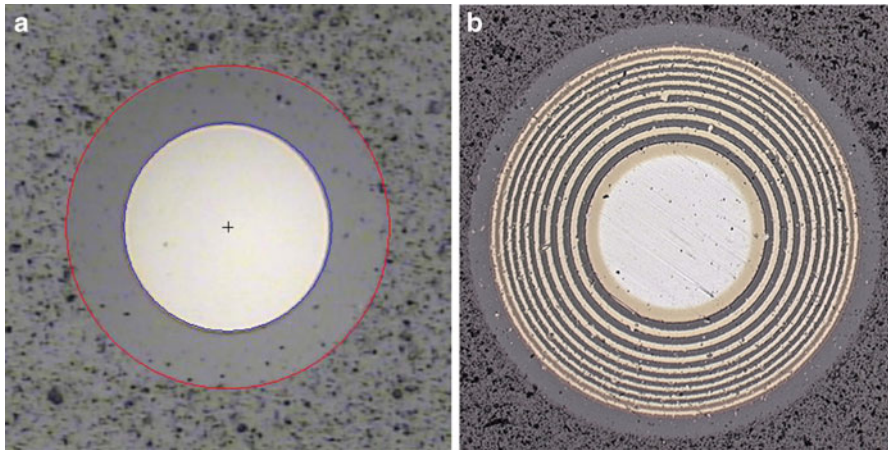
Fig. 4.26 Typical "calottes" made in (**a**) DLC monolayer coating on steel substrate and (**b**) multilayer of alternating TiN–TiCN coatings on steel substrate
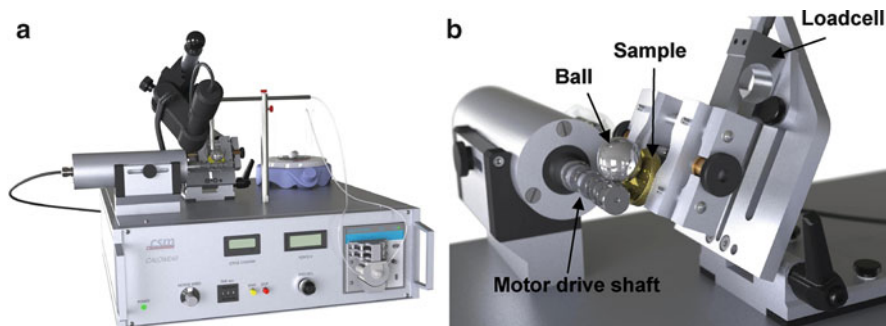
Fig. 4.27 Commercially available Calowear Tester (**a**) and detail of test setup (**b**)

Previous work [35] has shown that the ball crater wear behaviour of a wide range of Physical Vapour Deposition (PVD)-coated tool steels can be directly correlated to their performance as cutting tools. This means that the technique can be used to rank different cutting tool coatings for use in specific abrasive wear situations and also as a quality assurance tool in a production environment.

3 Examples of Tribology Testing Applications

The following examples are used to illustrate the use of some of the aforementioned tribology test methods in real applications.

3.1 High-Temperature Testing of TiN Coatings

Coatings used to extend the lifetime of cutting tools need to be tested at the temperatures at which they will be subjected in service.

In this study a CSM Instruments High Temperature Tribometer (capable of testing up to 1,000 °C) was used to carry out high-temperature wear testing of 2–3 μm thick TiN coatings applied on a steel K 110 steel substrate via Physical Vapour Deposition (PVD).

Figure 4.28 shows the High Temperature Tribometer which uses two linear variable differential transformer (LVDT) sensors for an accurate differential measurement of the tangential force without influence of temperature fluctuation (thermal drift). In practice, this means that the temperature gradient from the oven (surrounding the sample) to the measuring arm has no influence on the measurement of the coefficient of friction, even with significant temperature variations. A 6 mm diameter alumina ball was used as the static partner with a normal load 5 N
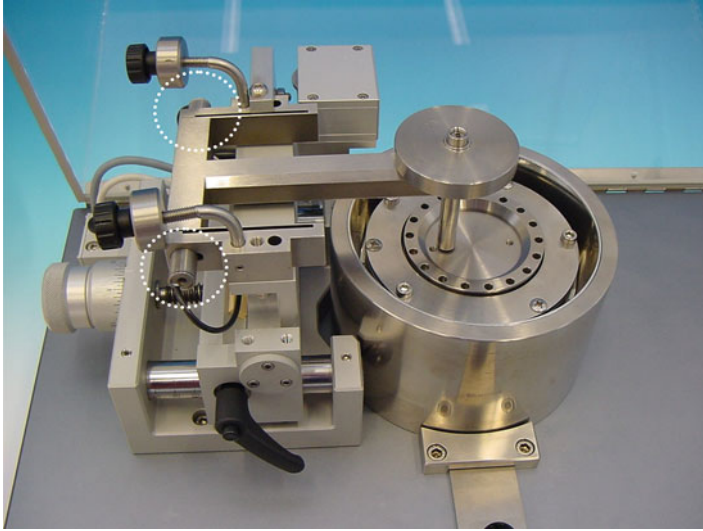
Fig. 4.28 CSM Instruments High Temperature Tribometer with two LVDT sensors (*circled*) which provide an accurate differential measurement of tangential force

Table 4.1 COF and wear measurements from high-temperature test of the TiN sample

|	25 °C	150 °C	300 °C	500 °C	750 °C
Coefficient of friction (COF)	0.383	0.597	0.655	0.809	0.91
Wear of the ball (μm)	400	370	350	340	600
Wear of the disk (h in μm)	1.35	1.5	1.65	5.9	1.6
Wear of the disk (area in μm^2)	350	400	450	780	65

and linear velocity of 10 cm/s. Wear testing was carried out at 25, 150, 300, 500, and 750 °C on TiN-coated samples.

The results from the tests shown in Table 4.1 and Fig. 4.29a indicate an increase in coefficient of friction with an increase in temperature. Figure 4.29b shows that the wear on the ball steadily decreased until 500 °C. Once the temperature reached 750 °C, the wear on the ball increased to 600 μm. There was an increase in the area of wear until 500 °C to 780 μm^2, but at 750 °C the wear area decreased to a minimal 65 μm^2. The decrease in wear can be attributed to the fact that TiN oxidizes at 600 °C which is confirmed by Fig. 4.30 which shows the visible surface oxide present at 500 and 750 °C. The hard oxide layer therefore decreases the wear of the coating.

An interesting observation was made during the wear tests of the TiN-coated steel. Whilst the COF of the TiN increased with the rise in temperature, the wear decreased beyond 500 ºC. This correlated to the oxidation of TiN which occurred around 600 ºC. This would suggest that TiN is a valid coating for high-temperature cutting applications where the surface oxide can extend the service lifetime significantly.
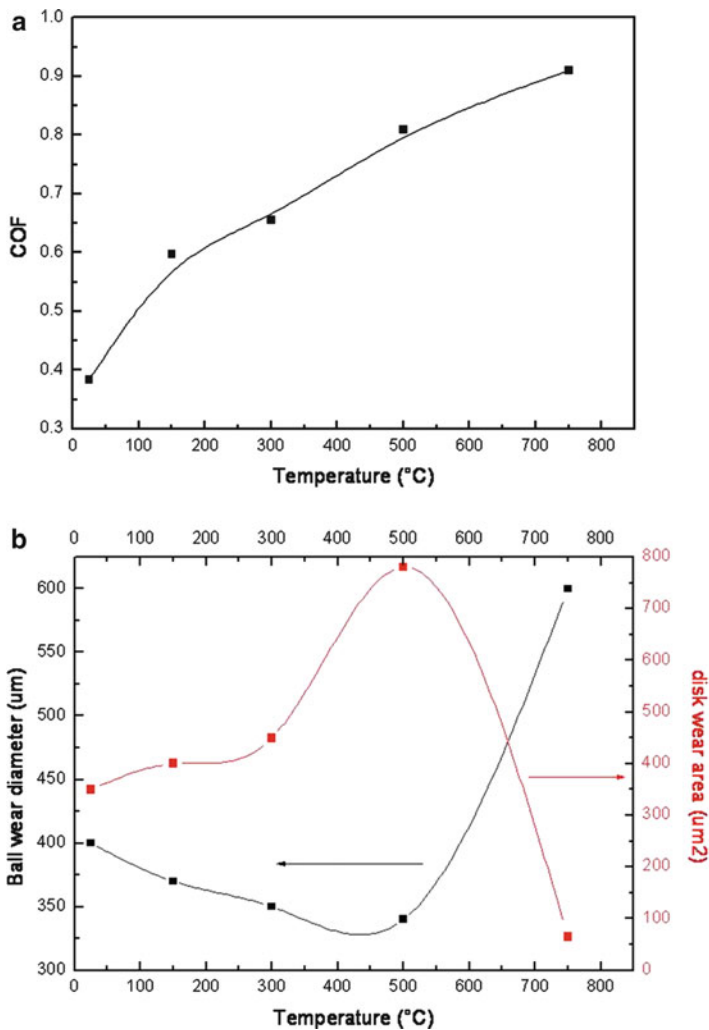
Fig. 4.29 (**a**) COF recorded during the high-temperature tests of the TiN-coated sample as a function of temperature. (**b**) Ball and disk wear recorded during the high-temperature tests of the TiN-coated sample as a function of temperature
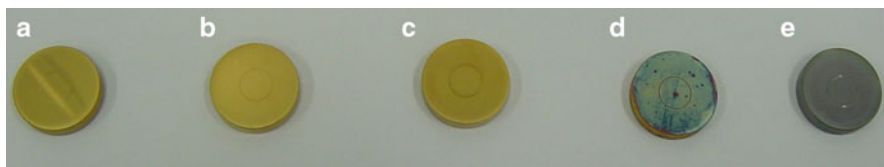
Fig. 4.30 TiN-coated samples after testing at temperatures of (**a**) 25 °C, (**b**) 150 °C, (**c**) 300 °C, (**d**) 500 °C, and (**e**) 750 °C

3.2 Lifetime Study of Automotive Wheel Bearings

In automotive applications, bearings form an integral part of many subassemblies, e.g. axle, engine, and gearbox, and their accurate characterization needs to take into account the final configuration of the bearing system. In the case of ball and tapered roller bearings, different types of loading may be applied at any one time, such as radial, axial, or other combination. The ratio of the radial to the axial load, the setting, and the bearing included cup angle determine the load zone in a given bearing. This load zone is defined by an angle which delimits the rollers or balls carrying the load. If all the balls are in contact and carry the load, then the load zone is referred to as being 360°.

Within the industry, the bearing life is defined as the length of time, or the number of revolutions, required to produce a fatigue spall of a size corresponding to an area of 6 mm^2. Such a lifetime will depend on many factors such as applied load, speed, lubrication, fitting, setting, operating temperature, contamination, maintenance, as well as environmental considerations. Due to all these factors, the life of an individual bearing is impossible to predict precisely, and experience has shown that several bearings which appear identical can exhibit considerable life scatter when tested under identical conditions.

The pin-on-disk tribometer has proved ideal for investigating the evolution of friction and wear in a wide range of typical bearings as a function of the axial load. Figure 4.31 shows a typical friction trace for a single row bearing after 1 million revolutions. The friction coefficient, μ, soon stabilizes after running-in, after which it gradually decreases. Other studies have shown that the value stabilizes after several million laps.

Specially fabricated holders are used to mount the bearing and outer casings (see Fig. 4.32), and the complete "sandwich" is supported in a modified support shaft. A flat pin is used to apply the static 50 N load as shown in Fig. 4.33.

The required load zone of the bearing can be varied by changing the contact area and lateral position of the pin in order to simulate in-service conditions more accurately.

## 3.3 In Vitro Testing of Orthopaedic Coatings

The laboratory testing of biomaterials is often the first step in being able to rank a particular type of material within a specific wear application. Once a suitable material has been evaluated fully at the laboratory scale, in controlled environmental conditions, the next stage may often be a clinical trial in either an animal or human patient.

Fig. 4.31 Friction coefficient versus number of laps (100,000×) for a single row bearing tested with the pin-on-disk tribometer. Note the initial running-in period and the gentle decrease in friction coefficient. Tests were carried out with an applied load of 50 N and speed 28 cm/s
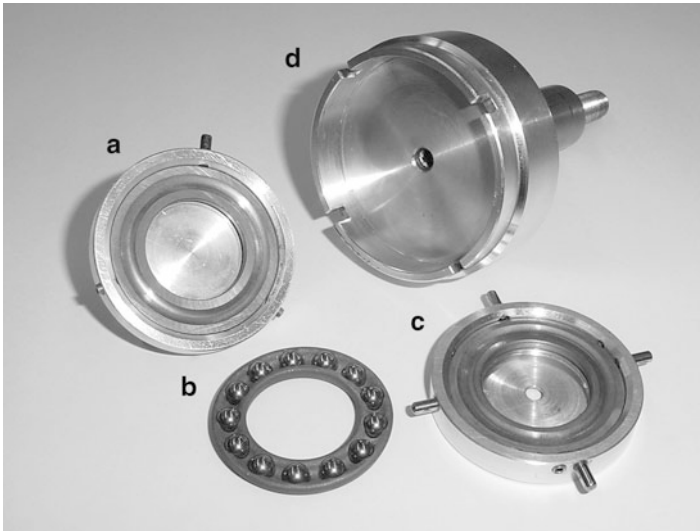

Fig. 4.32 The component parts of a single row bearing: upper casing (**a**), inner bearing (**b**), and lower casing (**c**) which is located in a specially modified sample support shaft (**d**)
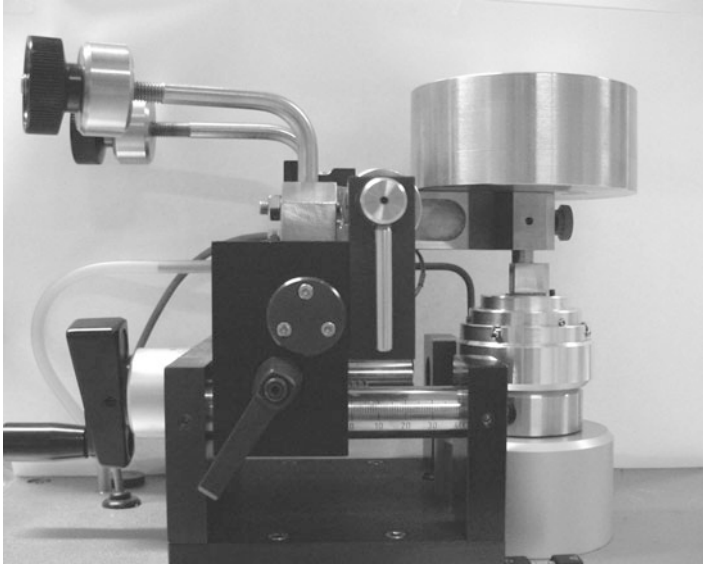
Fig. 4.33 The bearing shown was mounted on the tribometer for the test conditions summarized in Fig. 4.32

Tin oxide coatings are currently being developed for applications within the body where good adhesion and biocompatibility are the main considerations. Such coatings are spin coated onto standard stainless steel (316 L) substrates in a way that the coating thickness can be accurately controlled and the substrate roughness (R_{rms}) is less than 200 nm as verified by profilometry before deposition. The experimental setup consists of a pin-on-disk tribometer with a liquid cell and heating coil as shown in Fig. 4.34. The static partner is a 100Cr6 steel ball of diameter 6 mm and the materials in contact are submerged in BMF solution which is maintained at 37 °C for the duration of the test. The applied load is 2 N, linear speed 10 cm s^{-1}, and the wear radius is 3 mm.

The result of such a test is shown in Fig. 4.35 where an initial running-in period is followed by stabilization of the friction coefficient at a value of approximately 0.13 before increasing gradually until first failure of the coating occurs. As the coating starts to break down (after 2,730 revolutions), the friction coefficient drastically increases until at a value of 0.55 the substrate is reached and the coating no longer retains any integrity. Beyond about 4,000 revolutions the friction coefficient stabilizes at about 0.64. In this study, the test was paused at different points so that the sample could be imaged in a scanning electron microscope (SEM) to investigate the exact mode of failure and gain understanding about the amount of debris produced around the wear track.
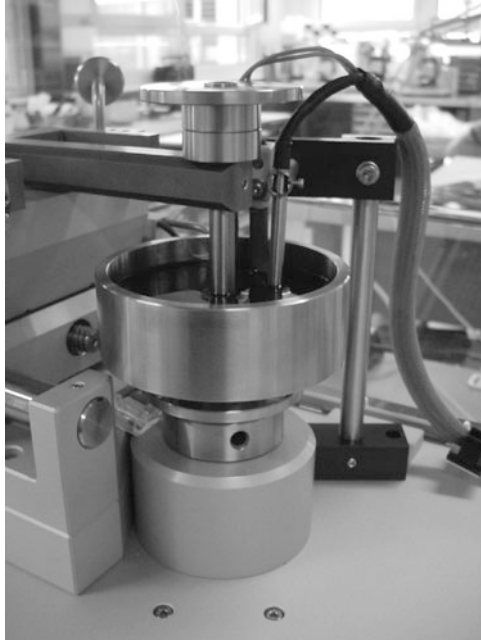
Fig. 4.34 Experimental setup for a tin oxide-coated 316 L steel disk in contact with a 100Cr6 steel ball, submerged in BMF and maintained at 37 °C with heating coil
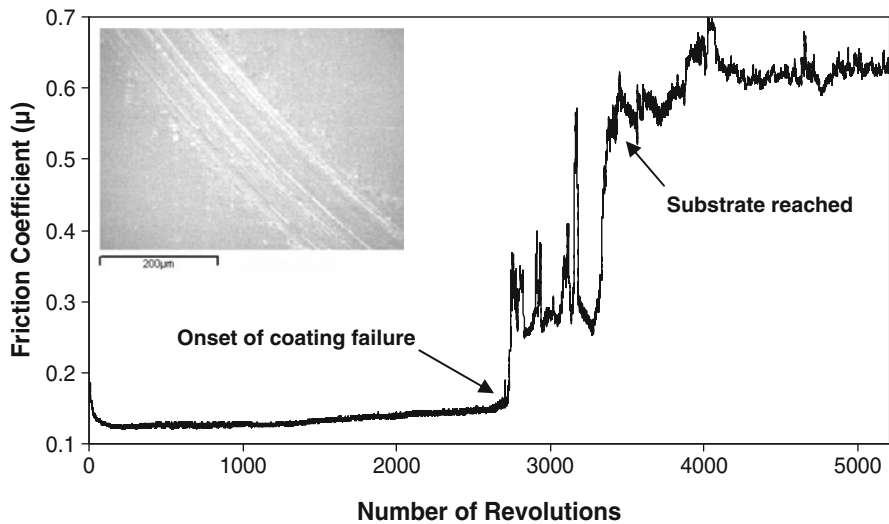
Fig. 4.35 Friction coefficient evolution for the test. The onset of coating failure and the point at which the substrate is reached are clearly denoted. SEM micrograph of the wear track confirms coating failure (*inset*)
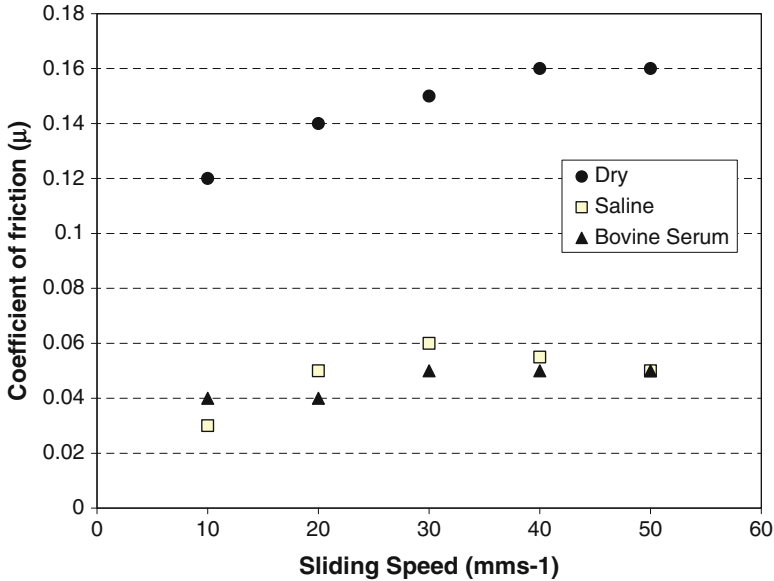
Fig. 4.36 Friction coefficients of a calcium phosphate coating (deposited on a steel substrate) when sliding against a UHMWPE pin at various different sliding speeds and in both dry and lubricated conditions

3.4 Dry and Wet Testing of Bone Biocompatible Coatings

Various biocompatible coatings have been developed in recent years for promoting fast healing between bone and a prosthetic implant material which may be ceramic, metallic, or polymeric (e.g. UHMWPE). Examples of such coatings are calcium phosphate and hydroxyapatite, both of which are found to have varying friction and wear properties when sliding in different environments. The results in Fig. 4.36 show the friction coefficients of a calcium phosphate coating (deposited on a steel substrate) when sliding against a UHMWPE pin at various different sliding speeds.

The experiment was repeated in dry and lubricated conditions. The two lubricants used were a standard saline solution (distilled water containing 0.1 % NaCl) and a commercially available bovine serum. Testing was performed on a pin-on-disk tribometer in unidirectional sliding (rotating) mode using an applied load of 2 N and a sliding speed from 10 to 50 mm s^{-1}, in 10 mm s^{-1} increments. At each speed condition, the average friction coefficient was calculated from data acquired over 30 min. In the dry condition, the friction coefficient increases from 0.12 at 10 mm s^{-1} up to 0.16 at 50 mm s^{-1}. In the saline and bovine serum lubricants, the friction coefficient drops to 0.03–0.06 with the bovine serum environment giving slightly lower values than the saline solution.

Fig. 4.37 Wear track of the
calcium phosphate coating
after 28 min of sliding at a
speed of 40 mm s^{-1} in dry
conditions
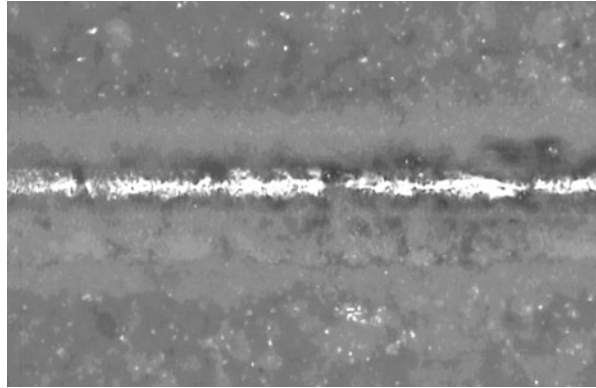
A typical wear track on the calcium phosphate coating is shown in the micrograph
in Fig. 4.37, and the wear debris can be seen along the edges and the steel substrate
has been reached.

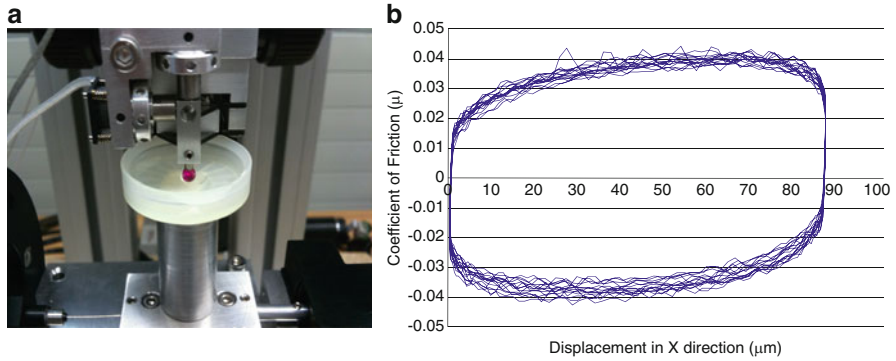## 3.5 Friction Study of Hydrogel Contact Lenses

The tribology testing of contact lens materials is usually performed under very low
contact pressure conditions so as to simulate the effect of the eyelid during blinking
which is of the order of 3.5–4.0 kPa with an average speed of approximately
12 cm s^{-1} [24–26]. Soft contact lenses are made of hydrogels which may contain
up to 75 % water, and the contact pressure encountered in the human eye can cause
redistribution and/or reduction of the water content, sometimes causing ocular
discomfort, such properties also being related to the frictional characteristics.
Testing of such soft contact lenses is therefore quite challenging as the applied
loads tend to be only a few mN and so a high-resolution instrument is required, such
as a CSM Instruments Nanotribometer 2. Contact lenses can be tested either with
the lens acting as the static partner (see Fig. 4.38) or with the lens mounted flat and
therefore operating as the dynamic partner (Fig. 4.39). In some cases, the lens may
be mounted as the dynamic partner but using a spherical substrate which matches
the curvature of the cornea. Typical experimental conditions might be an applied
load of 4 mN, frequency 0.2 Hz, and stroke length of 100 μm. The lens is usually
tested completely submerged in saline solution in order to prevent it drying out and
causing error in the measured friction coefficient.

Some experimental points which should be remembered when testing soft
contact lenses are that the friction coefficient may differ between the two sides of
the lens so it is important to always mount the lenses the same way. Secondly, there
must be no air bubbles between the lens and its mounting. Often the lens can be
secured to the substrate simply by capillary force, provided that the contact
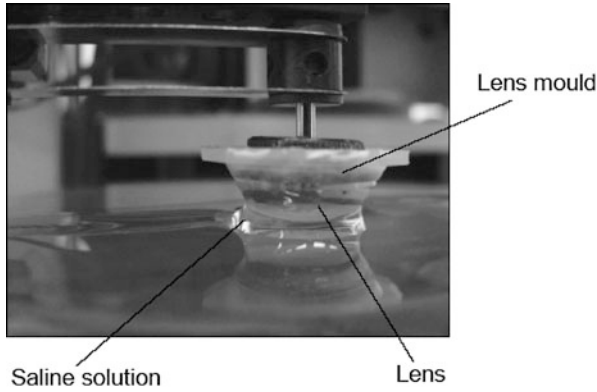
Fig. 4.38 Soft hydrogel contact lens mounted as the static partner on a nanotribometer and reciprocating linearly against a compliant substrate submerged in contact lens saline solution

Fig. 4.39 Schematic view of a soft hydrogel contact lens mounted flat in a liquid cup (**a**) and reciprocating against a ruby ball of diameter 3 mm. The results after 20 cycles are shown in (**b**) where the average coefficient of friction was 0.03

pressures used are not too high. Sometimes, the lenses may need to be properly clamped down. Care should be taken not to stretch or deform them during the mounting process.

References

1. Bowden F, Tabor D (1973) Friction: an introduction to tribology. Anchor Press/Doubleday, Garden City, NY
2. Hutchings IM (1992) Tribology: friction and wear of engineering materials. Edward Arnold, London

3. Holmberg K, Matthews A (1994) Coatings tribology: properties, techniques and applications in surface engineering. Tribology Series 28, Elsevier Science
4. ASTM G99: standard test method for wear testing with a pin-on-disk apparatus
5. ASTM G133: standard test method for linearly reciprocating ball-on-flat sliding wear
6. Bowden F, Tabor D (1964) The friction and lubrication of solids, part I (1950) and part II. Clarendon Press, Oxford
7. Briscoe BJ, Tabor D (1978) Friction and wear of polymers, polymer surfaces. Wiley, New York
8. Buckley DH (1981) Surface effects in adhesion, friction, wear and lubrication. Tribology Series No. 5, Elsevier
9. Ling FF, Pan CHT (1988) Approaches to modeling of friction and wear. Springer, New York
10. Rabinowicz E (1965) Friction and wear of materials. Wiley, New York
11. Fundamentals of Friction and Wear of Materials. Rigney DA, ed. (1981) Papers Presented at the 1980 ASM Materials Science Seminar, 4–5 October 1980, Pittsburgh, Pennsylvania, ASM, Ohio, pp 235–289
12. Singer IL, Pollock HM (1992) Fundamentals of friction. Kluwer, Dordrecht
13. Landolt D (2006) Electrochemical and materials aspects of tribocorrosion systems. J Phys D Appl Phys 39:1–7
14. Yan Y (2006) Biotribocorrosion—an appraisal of the time dependence of wear and corrosion interactions part II: surface analysis. J Phys D Appl Phys 39:3206–3212
15. Landolt D (2007) Corrosion and surface chemistry of metals. EPFL Press, Lausanne, Switzerland, pp 227–274
16. Mischler S, Ponthiaux P (2001) Wear 248:211–225
17. Azzi M, Szpunar JA (2007) Tribo-electrochemical technique for studying tribocorrosion behavior of biomaterials. Biomol Eng 24(5):443–446
18. Azzi M, Benkahoul M, Szpunar JA, Klemberg-Sapieha JE, Martinu L (2009) Tribological properties of CrSiN-coated 301 stainless steel under wet and dry conditions. Wear 267 (5–8):882–889
19. Azzi M, Amirault P, Paquette M, Klemberg-Sapieha JE, Martinu L (2010) Corrosion performance and mechanical stability of 316L/DLC coating system: role of interlayers. Surf Coatings Technol 204(24):3986–3994
20. Jalota S, Bhaduri SB, Cuneyt Tas A (2008) Using a synthetic body fluid (SBF) solution of 2 mM HCO_3 to make bone substitutes more osteointegrative. Mater Sci Eng C28:129–140
21. Baboian R (2005) Corrosion tests and standards: application and interpretation, ASTM manual series, MNL 20 ISBN 0-8031-2098-2
22. Laing PG (1977) Tissue reaction to biomaterials, NBS Special Publication 472, Gaithersburg MD, pp 31–39
23. ASTM F-732: standard test method for wear testing of polymeric materials used in total joint prostheses
24. Nairn JA, Jiangizaire T (1995) ANTEC '95, 3384
25. Freeman ME, Furey MJ, Love BJ, Hampton JM (2000) Wear 241:129
26. Rennie AC, Dickrell PL, Sawyer WG (2005) Friction coefficient of soft contact lenses: measurements and modeling. Tribol Lett 18(4):499–504
27. ASTM D5183: standard test method for determination of the coefficient of friction of lubricants using the four-ball wear test machine
28. ASTM D4172: standard test method for wear preventive characteristics of lubricating fluid (four-ball method)
29. ASTM D2266: standard test method for wear preventive characteristics of lubricating grease (four-ball method)
30. ASTM G65: standard test method for measuring abrasion using the dry sand/rubber wheel apparatus
31. ISO EN-1071-2: determination of the abrasion resistance of coatings by a micro-abrasion wear test

32. Rabinowicz E, Dunn LA, Russel PG (1961) Wear 4:345
33. Rutherford KL, Hutchings IM (1996) Surf Coat Tech 79:231
34. Archard JF (1953) J Appl Phys 24:981
35. Rutherford KL, Bull SJ, Doyle ED, Hutchings IM (1996) Surf Coat Tech 80:176–180

Questions for Students

1. Name 6 typical tribometer configurations.
2. What is the difference between *steady state* and *static* friction coefficients?
3. Name 2 methods commonly used to determine the wear rate of a tested material.
4. What are the main components of a practical tribocorrosion setup and what are the 3 modes of operation?
5. What are the 3 most common parameters measured with the four-ball wear tester?
6. What is the main parameter measured with the ball crater abrader?